I&EC research
Industrial & Engineering Chemistry Research

Separations

Polyamide/MOF Bilayered Thin Film Composite Membranes for the Removal of Pharmaceutical Compounds from Water

Lorena Paseta, Daniel Antorán, Joaquin Coronas, and Carlos Téllez

Ind. Eng. Chem. Res., **Just Accepted Manuscript** • DOI: 10.1021/acs.iecr.8b06017 • Publication Date (Web): 20 Feb 2019

Just Accepted

ACS Publications

is published by the American Chemical Society. 1155 Sixteenth Street N.W., Washington, DC 20036

110th Anniversary: Polyamide/MOF Bilayered Thin Film Composite Membranes for the Removal of Pharmaceutical Compounds from Water

*Lorena Paseta†, Daniel Antorán†, Joaquín Coronas†‡, Carlos Téllez†‡**

†Instituto de Nanociencia de Aragón (INA) and Chemical and Environmental Engineering Department, Universidad de Zaragoza, 50018 Zaragoza, Spain.

‡ Instituto de Ciencia de Materiales de Aragón (ICMA), CSIC-Universidad de Zaragoza, 50018 Zaragoza, Spain

*Corresponding author: ctellez@unizar.es

ABSTRACT: Nanofiltration can be a useful tool to remove pharmaceuticals in water sources. The performance of the most used Thin Film Composite (TFC) membranes, typically with a thin polyamide (PA) layer, can be improved using Thin Film Nanocomposite (TFN) membranes obtained by the introduction of a filler within the PA layer. In this work, to control the positioning of the filler two kinds of PA/MOF Bilayered TFC (BTFC) membranes, PA/ZIF-93 and PA/HKUST-1, were synthesized onto polyimide supports. First, the interfacial synthesis was used for the preparation of a MOF layer, and second, a PA layer was synthesized by interfacial polymerization. These BTFC membranes

were applied in the nanofiltration of Diclofenac and Naproxen aqueous solutions obtaining a maximum water permeance of 33.1 and 24.9 $L \cdot m^{-2} \cdot h^{-1} \cdot bar^{-1}$, respectively, with a rejection ≥98 % when HKUST-1 was used. These permeance improvements (using Diclofenac, 4.9 and 3.4 times the value of the TFC and TFN membranes, respectively) are related to the PA layer thickness, MOF porosity, membrane hydrophilicity and membrane roughness.

KEYWORDS: Interfacial synthesis, pharmaceuticals removal, nanofiltration, Polyamide/MOF bilayer, Metal-Organic frameworks

INTRODUCTION

A current environmental problem is the presence of so-called micro-pollutants or emerging contaminants present in wastewater treatment plant (WWTP) effluents, surface water, ground water and even drinking water. WWTPs are not capable of removing these micro-pollutants effectively.[1,2] These contaminants include pharmaceuticals, which are not completely assimilated by the organism and end up in the aquatic environment causing negative effects on the human and ecological health.[3,4] For example in effluents of WWTP located in the Ebro River basin, where the University of Zaragoza is placed, Diclofenac and Naproxen were detected up to levels of 1.1 $\mu g \cdot L^{-1}$ and 1.7 $\mu g \cdot L^{-1}$, respectively, the total pharmaceutical concentration being about 0.02 $mg \cdot L^{-1}$.[5] Several research studies have examined the use of membrane technologies as effective processes to remove micro-pollutants from water.[6,7]

Nanofiltration has become an interesting membrane separation process in a wide range of fields (pharmaceuticals,[8] food,[9] textile,[10] drinking water,[11] etc.) due to its low consumption of energy and low-cost maintenance in comparison with other separation processes such as

distillation[12] or reverse osmosis[13] for both aqueous and organic streams. Thin film composite (TFC) membranes are the most commonly used in this application, consisting of a non-woven fabric at the bottom that gives mechanical stability to the whole ensemble, an asymmetric polymeric support (usually made by phase inversion) and a selective ultrathin film layer at the top, synthesized by interfacial polymerization.[12]

One way to increase the flux of these membranes without sacrificing rejection is the introduction of nanoparticles during the interfacial polymerization of polyamide, resulting in the so-called "thin film nanocomposite" (TFN) membranes[14]. A wide variety of nanoparticles has already been used for this purpose: zeolites,[15] metal-organic frameworks,[16] graphene oxide,[17] and TiO_2,[18] among others.

Metal-organic frameworks (MOFs) are hybrid materials formed by the union of metal clusters with organic ligands.[19] They have been reported as interesting materials for the production of TFN membranes because their chemical variety (e.g. depending on the nature of the linker they can be hydrophilic or hydrophobic) and high porosity results in improvements in the performance of the membrane, e.g. increasing flux in nanofiltration processes.[16,20]. However, sometimes, agglomerates of MOFs can be formed during their dispersion in the organic solution that participates in the interfacial polymerization reaction. This may create non-selective defects between the polyamide and the MOF nanoparticles producing a decrease in the membrane performance. [20] In order to solve this problem, different methodologies to control the MOF positioning in the membrane have been developed: dip-coating,[21] layer by layer,[22] Langmuir-Blodgett[23] or evaporation-controlled filler positioning.[24].

To control the MOF positioning, we report here the synthesis of Polyamide/MOF Bilayered Thin Film Composite (PA/MOF BTFC) membranes on top of asymmetric polyimide supports. The MOF film is synthesized on the top of polyimide by interfacial synthesis method and then the polyamide film is synthesized by interfacial polymerization on top of the MOF film. To increase water permeance, two hydrophilic MOFs were selected: ZIF-93 and HKUST-1. ZIF-93 (Zn(4-methyl-5-imidazolecarboxaldehyde)$_2$) is a hydrophilic MOF belonging to the subclass known as "Zeolitic Imidazolate Framework". It is formed by the coordination of Zn cations with 4-methyl-5-imidazolecarboxaldehyde resulting in a "**rho**" topology with a pore size of 3.6 Å.[25] HKUST-1, also hydrophilic like ZIF-93, was one of the first MOFs reported.[26] With the empirical formula $Cu_3(BTC)_2(H2O)_3$ (where BTC is 1,3,5-bencenetricarboxylate), HKUST-1 has a face-centered-cubic structure and a pore size of 6-9 Å.[26] The membranes obtained were applied in the nanofiltration process for the removal of pharmaceuticals, specifically Diclofenac and Naproxen, two analgesics in common daily use and whose presence has even been found in drinking water.[27,28]

EXPERIMENTAL

Synthesis of MOF powders

The synthesis of ZIF-93 was carried out as previously reported,[29] while the synthesis of HKUST-1 followed the same procedure as described by Wee et al.[30]

Preparation of PI supports.

The PI supports were prepared as follows: a dope solution of 24% (w/w) was obtained by dissolving P84® (HP polymer GmbH) in DMSO (99.5%, Scharlab) and stirring overnight. Once dissolved, the solution was allowed to stand until the air bubbles disappeared. The

solution was then cast on a polypropylene non-woven backing material (Freudenberg Performance Materials) at a casting speed of 0.04 $m \cdot s^{-1}$ using a casting knife set (Elcometer 4340 Automatic Film Applicator), at a thickness of 250 µm. Immediately after casting, the membrane was immersed in a deionized water bath, where the phase inversion occurred. After 10 min, membranes were transferred to a fresh water bath and left for 1 h. The wet membranes were then immersed in two consecutive baths of isopropyl alcohol (IPA – 99.5%, Scharlab) of 1 h each to remove any residual water or DMSO. The supports were cross-linked by immersing them in a 120 $g \cdot L^{-1}$ solution of hexanediamine (HDA – 98%, Sigma Aldrich) in IPA for 16 h at 20°C. Next, the membranes were washed with IPA four times for 1 h each to remove any traces of HDA. Finally, the supports were immersed in a solution with a 3:2 volume ratio of polyethylene glycol (PEG – synthesis grade, Scharlab): IPA overnight to prevent the pores from collapsing and as well as the formation of PA inside them during the interfacial polymerization (IP) reaction.[16,20]

Preparation of TFC and TFN membranes

TFC and TFN were prepared on cross-linked P84® supports by interfacial polymerization. For this purpose, a 60.8 cm^2 support disk was placed in a glass filtration holder for the IP reaction and 30 mL of an aqueous solution of 2% (w/v) m-phenylenediamine (MPD, 99%, Sigma-Aldrich) was poured over the support and left for 2 minutes. After this time, the excess solution was removed and the membrane was wiped with tissue paper. Then, 30 mL of a solution of 0.1% (w/v) trimesoyl chloride (TMC, 98%, Sigma-Aldrich) was added and after 1 minute of reaction, 10 mL of hexane was added to stop the reaction. Then, 10 mL of hexane was added to remove the unreacted TMC and finally 10 mL of deionized water was added to wash the hexane. The obtained TFC membrane was stored in deionized water. In

the case of TFN, the procedure followed was the same as above, except that 0.2% (w/v) of synthesized MOF was dispersed in the organic phase before the IP reaction.

Synthesis of Polyamide/MOF Bilayered Thin Film Composite (PA/MOF BTFC) Membranes

The synthesis of the PA/HKUST-1 BTFC membrane was done following a procedure similar to that used by Campbell et al.[31] Firstly, a 60.8 cm^2 porous PI support disk was placed in a glass filtration holder and a solution of 3.5 g of $Cu(NO_3)_2 \cdot 2.5H_2O$ (98%, Alfa Aesar) in 50 mL of deionized water was poured and left overnight. After this time, the excess solution was removed and the membrane was wiped with tissue paper. Then, a solution of 0.85 g of trimesic acid (98%, Alfa Aesar) in a mixture of 50 mL of octanol (99%, Alfa Aesar) and 15 mL of methanol (HPLC grade, Scharlau) was added and left to react during 1 min, after which the supernatant was taken away and the membrane was washed with methanol and dried under ambient conditions. A second polyamide thin layer was then synthesized at the top of the HKUST-1 layer by the interfacial polymerization process described above.

In the case of the PA/ZIF-93 BTFC membrane, the same methodology used for the synthesis of HKUST-1 was followed but in this case the aqueous phase was a solution of 2.23 g of $Zn(NO_3)_2 \cdot 6H_2O$ (98%, Scharlau) in 50 mL of deionized water and the organic phase was a solution of 1.65 g of 4-methyl-5-imidazolecarboxaldehyde (97%, Maybridge) and 1.02 g of sodium formate (99%, Sigma-Aldrich) in a mixture of 40 mL of methanol and 20 mL of octanol. The reaction time was also 1 min.

Before the measurements, two post-treatments were applied to all the synthesized membranes (TFC, TFN, PA/HKUST-1 BTFC and PA/ZIF-93 BTFC membranes). The first consisted of washing in 50 mL of DMSO during 10 min at room temperature and the second consisted of filtering DMSO for 10 minutes at 20 bar and at room temperature. As Solomon et al.[32] demonstrated in their work, the post-treatment of the membranes with solvents like DMF or DMSO produces an enhancement of the membrane flux due to the removal of small molecular PA fragments.

Characterization

X-ray diffraction analysis (XRD) was performed with a D-max 2500 Rigaku diffractometer with a Cu Kα (λ=1.1542 Å) rotating anode, at 40 kV and 80 mA.

Scanning electron microscopy (SEM) and EDS were carried out with a FEI-Inspect F20 microscope operated at 10 kW. For the cross-sectional images, the samples were prepared by freeze-fracturing in liquid N_2. All samples were coated with platinum under vacuum conditions.

Both the MOFs and synthesized membranes were characterized by attenuated total reflection Fourier transform infrared spectroscopy (ATR-FTIR). The spectra were recorded in the 4000-600 cm^{-1} wavenumber range with an accuracy of 4 cm^{-1}. The equipment used was a Bruker Vertex 70 FTIR spectrometer equipped with a deuterated triglycine sulfate detector and a Golden Gate diamond ATR accessory.

Thermogravimetric analyses (TGA) were carried out using a TGA/SDTA 851e system (Mettler Toledo). The samples were heated up to 700 °C with a heating rate of 10 °C·min^{-1} under an air flow of 80 cm^3(STP)·min^{-1}.

The specific surface area and pore volume of the synthesized HKUST-1 and ZIF-93 nanoparticles were obtained using a Micrometrics Tristar 3000 at 77 K. The samples were first degassed at 200 °C for 8 h. Their specific surface areas were calculated by the Brunauer–Emmett–Teller (BET) method and the pore volume at a relative pressure of P/P_0=0.98.

The synthesized membranes were characterized by contact angle measurements using a Krüss DSA 10 MK2 at 20 °C. The measurements were done in three different places for each sample.

Membranes were characterized using atomic force microscopy (AFM), by means of a Veeco MultiMode 8 scanning probe microscope, in tapping mode under ambient conditions. A silicon cantilever provided by Bruker with a resonant frequency of 300 kHz and a force constant of 40 mN was used. Images were recorded at a scan rate of 1 Hz and an amplitude set-point lower than 1 V. The roughness average (R_a) and the root mean square (*RMS*) were obtained to compare the roughness between membranes.

Water nanofiltration

Nanofiltration experiments were carried out with a dead-end membrane module (Sterlitech HP4750). The performance of the membrane was assessed by using two different solutions: 1 mg·L^{-1} of Naproxen ((S)-(+)-2-(6-methoxy-2-naphthyl)propionic acid, 230.26 Da) (NAP-98%, Fluorochem) and 1 mg·L^{-1} of Diclofenac (2-[2-(2,6-dichloroanilino)phenyl]acetic acid, 296.15 Da) (DCL-98%, TCI) in water. Both concentrations were chosen in order to facilitate the detection. The effective area of the membrane was 12 cm^2 and the experiments were carried out at 20 °C and 20 bar under continuous stirring. The stability tests were

performed at 10 bar to prolong them. The membrane permeance and the rejection were calculated according to the following equations:

$$Permeance = \frac{V}{\Delta P \cdot A \cdot t} \quad (1)$$

$$Rejection\ (\%) = \left(1 - \frac{C_{permeate}}{C_{residue}}\right) \cdot 100 \quad (2)$$

where V is the permeate volume (L), A the membrane nanofiltration area (m^2), t the time for permeate collection (h) (1 min once the permeance was stable) and ΔP the pressure across the membrane (bar). The concentration of residue ($C_{residue}$) and permeate ($C_{permeate}$) were both measured by a Waters HPLC system with a UV-vis detector set at a wavelength of 284 nm for both pharmaceuticals.

RESULTS AND DISCUSSIONS

Characterization of the MOF particles for TFN membranes

The crystalline structures of ZIF-93 and HKUST-1 were confirmed by X-ray diffraction (see Figure S1). SEM images showed the characteristic morphologies described in the literature for both MOFs [29,30] (Figure S2) besides an adequate particle size: 800±170 nm in the case of HKUST-1 and 67±13 nm for ZIF-93. The thermal stability was determined by TGA (see Figure S3) showing no traces of solvent or unreacted linkers inside the pores and therefore both MOFs were well activated. Table 1 shows some selected properties of the two MOF powders used to prepare the TFN membranes.

Table 1: Crystal size (calculated measuring at least 50 particles helper by the software Vision Builder.), BET area and pore volume (at a relative pressure of P/P_0=0.98) of the HKUST-1 and ZIF-93 powders synthesized in this work for TFN membranes. The crystallographic pore size (Å) has been indicated as a reference.

MOF	Particle Size (nm)	BET surface area ($m^2 \cdot g^{-1}$)	Pore volume ($cm^3 \cdot g^{-1}$)	Pore/cavity diameter (Å)
HKUST-1	800±170	1378[33]	0.33	6/9[26]
ZIF-93	67±13	737±11	0.62	3.6[25]

Membrane characterization

TFN membranes were synthesized in order to compare their performance with the PA/MOF BTFC membranes and corroborate the improvement obtained with the latter.

SEM was carried out with both kinds of membranes. Figure 1a,d shows images before the IP, where it is possible to see that the synthesis of the MOF was carried out over the support surface. In the case of HKUST-1, a homogeneous film of MOF was synthesized, whereas in the case of ZIF-93 some areas appear uncoated. After the IP (Figure 1b,e), the PA/ZIF-93 BTFC membrane shows the typical ridge and valley morphology coating the whole MOF film. In case of PA/HKUST-1 BTFC membrane, the PA film seems to be thinner as seen in Figure 1b, where it is possible to distinguish a hole made during the SEM analysis. Namvar-Mahboub et al.[34] saw that the thickness of the polyamide layer decreased on TFN membranes when the filler loading increased in the PA layer due to the filler restricting the MPD diffusion to the organic phase, thus decreasing the polymerization reaction to form the PA layer. The same phenomenon was described by Wang et al.[22] when

they increased the number of layers of ZIF-8 synthesized over a support by the layer by layer method. Figure 1c,f shows the cross-sectional SEM images corresponding to PA/MOF BTFC membranes before IP where it can be observed that the MOF layer thickness is larger for HKUST-1 (≈1.5 μm) than for ZIF-93 (≈500 nm).

SEM images for the TFN membranes can be seen in Figure S4. For both MOFs, the membranes show the ridge and valley structures indicating that the PA layer has been correctly formed.

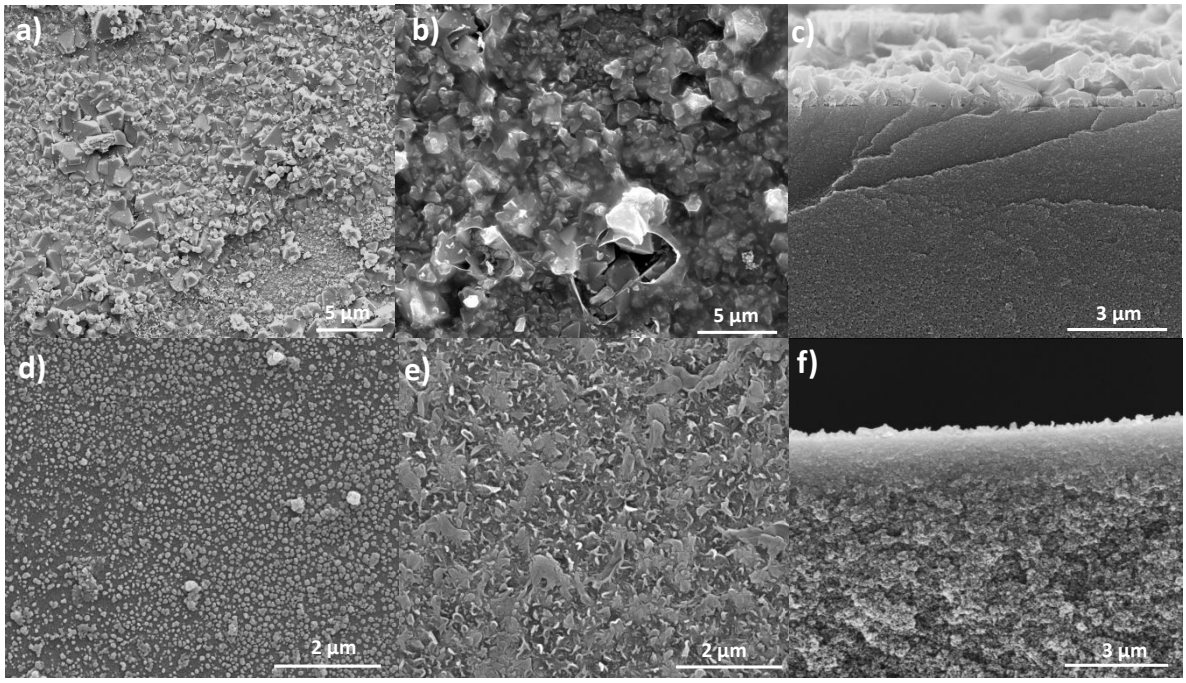

Figure 1: SEM images of different stages of preparation of PA/MOF BTFC Membranes. **a, b, c)** HKUST-1 before IP, after IP and cross-sectional before IP, respectively, and **d, e, f)** ZIF-93 before IP, after IP and cross-sectional before IP, respectively.

The ATR-FTIR spectra of the PA/MOF BTFC membranes and TFN membranes are shown in Figure 2 and Figure S5, respectively. Peaks related to the PA layer formation appear at

1639 cm^{-1} (amide I, C=O stretching vibration), 1537 cm^{-1} (amide II, C-N stretching) and 1465 cm^{-1} and 1405 cm^{-1} (amide functionalities, -NHCO- bond).[32] Regarding the PA/HKUST-1 BTFC sample, these peaks are less intense due to the fact that, as seen in SEM images (Figure 1b), the PA layer is thinner than for PA/ZIF-93 BTFC. In addition, new peaks appear in the PA/MOF BTFC and TFN membranes (more clearly after subtraction of the TFC membrane spectrum) corresponding to the characteristic peaks of the MOFs. In the case of the PA/HKUST-1 BTFC membrane, the bands at 1448 and 1371 cm^{-1} and at 760 and 729 cm^{-1} correspond to the COO-Cu_2 and C-CO_2 stretching vibrations, respectively.[35] Whereas in the PA/ZIF-93 BTFC membrane, the peaks at 1492 and at 1163 cm^{-1} correspond to the C=C and C-N stretching mode, respectively, and at 1028 and at 816 and 783 cm^{-1} are related to the C-H in plane and C-H out of plane bending, respectively.[36] This reveals their correct synthesis and that no structural changes occurred during the PA layer formation by interfacial polymerization.

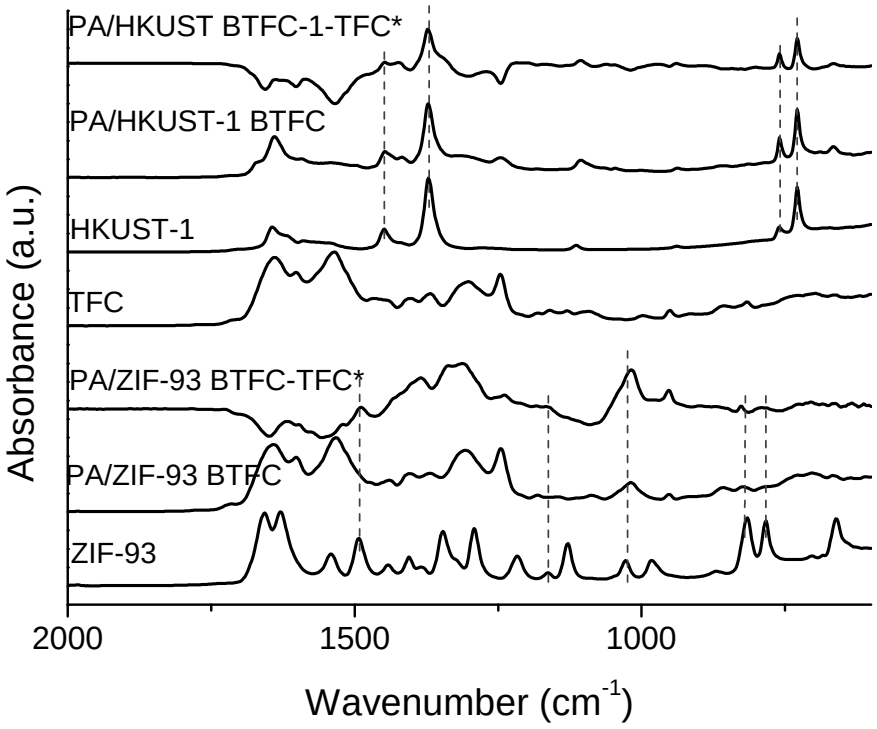

Figure 2: ATR-FTIR analysis of MOFs, TFC membrane and PA/MOF BTFC membranes. *ATR-FTIR spectra of the PA/MOF BTFC membranes after subtracting the TFC membrane spectrum.

Table 2 shows the contact angle values for the TFC, TFN and PA/MOF BTFC membranes. The measured contact angles follow a trend marked according to the added MOFs. Both MOFs are hydrophilic so the contact angle in the TFN and PA/MOF BTFC membranes decreased compared to the TFC membranes. The most hydrophilic membranes are those with HKUST-1. The TFN membranes for both MOFs are more hydrophilic than the PA/MOF BTFC membranes due to the fact that the nanoparticles in the former are more exposed to the membrane surface, while in PA/MOF BTFC the MOF layer was buried below the polyamide.

Table 2: Contact angle measurements.

	Contact Angle (°)
TFC	78±1
TFN ZIF-93	64±4
PA/ZIF-93 BTFC	71±3
TFN HKUST-1	51±3
PA/HKUST-1 BTFC	55±3

AFM images and derived R_a and *RMS* values of TFN MOF, PA/MOF BTFC and conventional TFC membranes are given in Figure 3. Independently of the type of MOF, the roughness is higher in the following order MOF/PA BTFC > TFN MOF > TFC membranes. The effect is more abrupt when the MOF HKUST-1 is used. Compared to the TFC membrane *(*R_a = ±12), the filler HKUST-1 within the polyamide layer in the TFN MOF membrane (R_a = ±144) increases the membrane roughness, in agreement with the literature.[23] The PA/HKUST-1 BTFC membrane (R_a = ±526) produced the highest roughness value. On the other hand, the PA/ZIF-93 BTFC membrane shows a lower roughness value (R_a = ±28) than its analog of HKUST-1 (R_a = ±526) due to what has already been observed by SEM (also obvious in the AFM images) of a ZIF-93 layer with no covered areas. The increase in the roughness of the membrane surface is a factor that causes an increase in the effective membrane area and therefore can play a key role increasing the permeance.

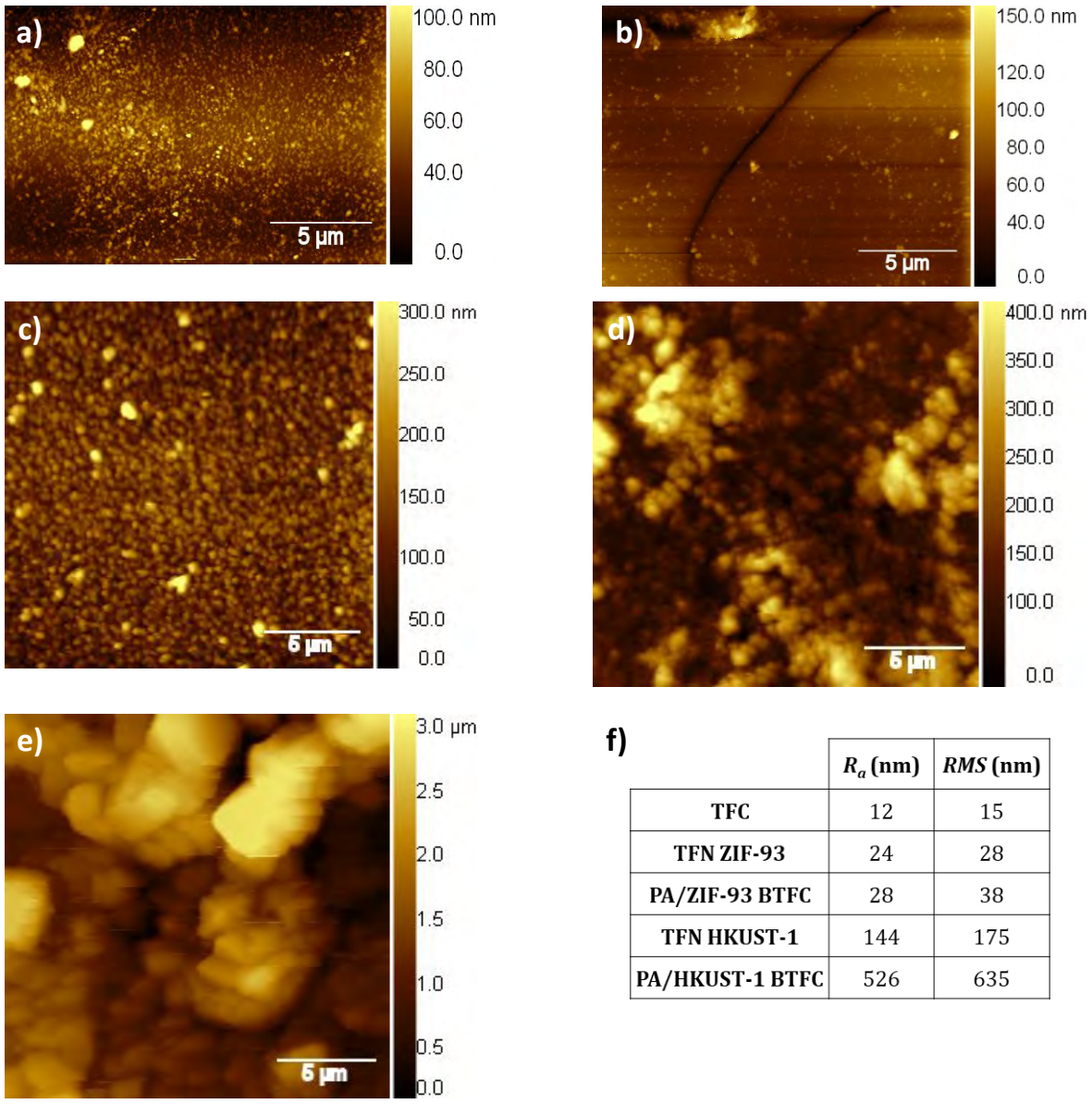

f)

	R_a (nm)	*RMS* (nm)
TFC	12	15
TFN ZIF-93	24	28
PA/ZIF-93 BTFC	28	38
TFN HKUST-1	144	175
PA/HKUST-1 BTFC	526	635

Figure 3: 2D AFM images of the top surface of **a)** TFC, **b)** TFN ZIF-93, **c)** PA/ZIF-93 BTFC, **d)** TFN HKUST-1 and **e)** PA/HKUST-1 BTFC membranes, and **f)** R_a and *RMS* values.

Results of Diclofenac and Naproxen aqueous solution nanofiltration

First, nanofiltration was carried out using Diclofenac as the solute (296.15 Da). The results obtained can be seen in Figure 4a and table S1. The rejection values obtained in all cases

were > 99 %. As has been observed previously in other studies, the insertion of filler particles giving rise to TFN membranes improves the membrane permeance in comparison to TFC membranes.[16,20] In this case an additional important improvement was achieved with the PA/HKUST-1 BTFC membrane compared with the TFN membrane containing HKUST-1 particles from 6.8 $L \cdot m^{-2} \cdot h^{-1} \cdot bar^{-1}$ for the TFC membrane to 33.1 $L \cdot m^{-2} \cdot h^{-1} \cdot bar^{-1}$ for the PA/MOF BTFC membrane of water permeance, whereas the Diclofenac rejection was ≥99%. Fig. 4a depicts analogous results with ZIF-93, the water permeance being 24.2 $L \cdot m^{-2} \cdot h^{-1} \cdot bar^{-1}$ and the rejection ≥99%.

This increase in permeability compared to TFC membranes (calculated as $(P_{PA/MOF}-P_{TFC})/P_{TFC} \cdot 100$) in PA/HKUST-1 BTFC (>380%) and in PA/ZIF-93 BTFC (>255%) is related to the porosity of the MOF, the higher hydrophilicity of the membranes and the higher surface roughness. These three parameters are higher for PA/HKUST-1 BTFC than for PA/ZIF-93 BTFC membranes (see tables 1 and 2 and Figure 4f) explaining the difference between both MOFs. Regarding the permeance, other factor should be taken into account such as the lower thickness of the polyamide layer in the PA/HKUST-1 BTFC membrane.

Once it was established that the best performances were obtained with PA/MOF BTFC membranes, with the continuous layer of MOF coated with polyamide, these membranes were used in the nanofiltration of Naproxen (230.26 Da) aqueous solution. The best performance for the nanofiltration of Naproxen aqueous solution was obtained with HKUST-1 (Figure 4b and Table S1), with an increase in the water permeance from 4.3 $L \cdot m^{-2} \cdot h^{-1} \cdot bar^{-1}$ for the TFC membrane to 24.9 $L \cdot m^{-2} \cdot h^{-1} \cdot bar^{-1}$ for the PA/HKUST-1 BTFC membrane. The flow also using the PA/ZIF-93 BTFC membrane reached values of 10.5

$L \cdot m^{-2} \cdot h^{-1} \cdot bar^{-1}$. In this case, the rejection decreased somewhat from 99.3% for the TFC to 98.3% for the PA/HKUST-1 BTFC while it was maintained for the PA/ZIF-93 BTFC. The lower size of Naproxen compared to Diclofenac should be taken into account and, as can be seen in Table 1, the pore size of HKUST-1 is larger than that of ZIF-93. Thus, Naproxen can diffuse more easily.

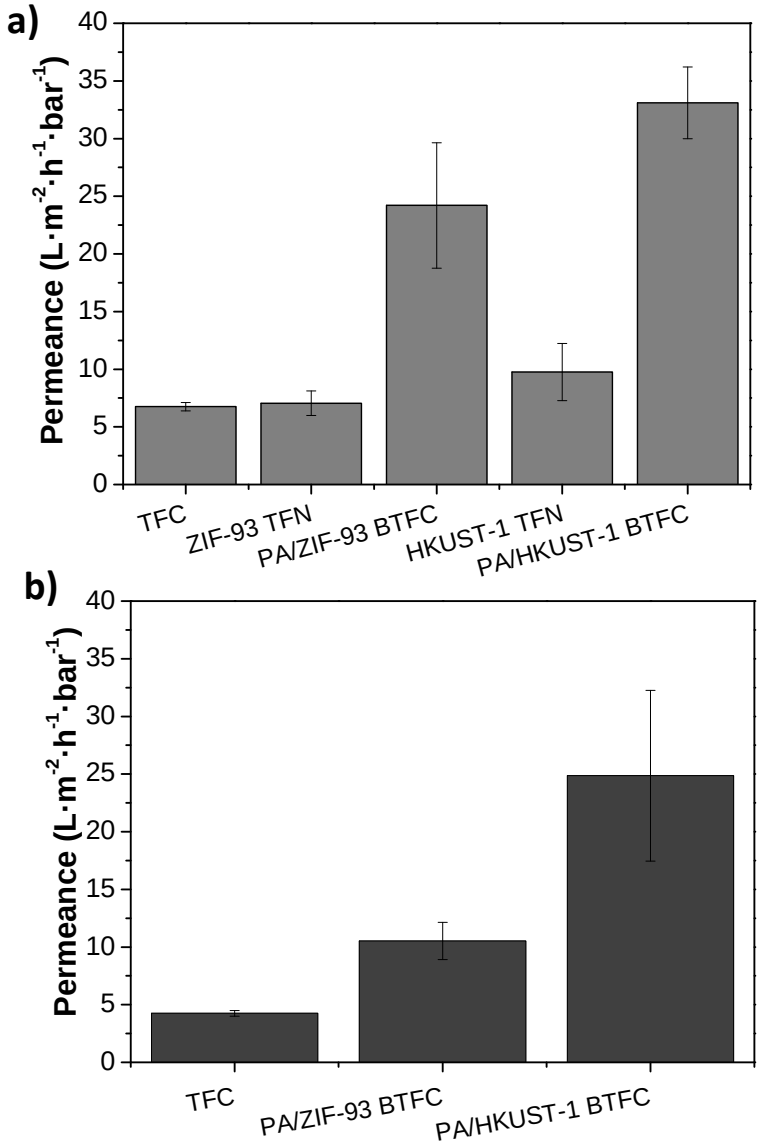

Figure 4: Nanofiltration performance using as solute: **a)** Diclofenac and **b)** Naproxen. The values given are an average of three membranes. Applied pressure 20 bar and temperature 20 ºC. The rejection values obtained in all experiments were > 98% (see table S1).

The water permeances obtained in the nanofiltration of Diclofenac aqueous solution are higher than in the case of Naproxen aqueous solution. This is true with all the three types of membrane (TFC, TFN and PA/MOF BTFC). This suggests that some fouling ocurred when Naproxen was used as the solute in the nanofiltration proccess. The Hansen Solubility Parameters (HSP) are useful for gaining insight into the fouling phenomenon.[16] Table 3 shows the HSP of Diclofenac, Naproxen and polyamide (PA).

Table 3: Differences in the Hansen solubility parameters (Ra) calculated as described by Hansen,[37] obtained by for each pharmaceutical[38] and PA[16], where each HSP correspond to a specific interaction: δ_D refers to the dispersion forces, δ_P to the dipolar forces and δ_H is due to the contribution of the hydrogen bonds.

	δ_D ($MPa^{0.5}$)	δ_P ($MPa^{0.5}$)	δ_H ($MPa^{0.5}$)	Ra ($MPa^{0.5}$)[a]
Diclofenac	16.27	18.05	13.48	9.00
Naproxen	17.35	12.14	9.86	2.36
PA	18.0	11.9	7.9	0.00

[a]Calculated according to $Ra^2 = 4(\delta_{D1} - \delta_{D2})^2 + (\delta_{P1} - \delta_{P2})^2 + (\delta_{H1} - \delta_{H2})^2$ where δ_{D1}, δ_{P1} and δ_{H1} and δ_{D2}, δ_{P2} and δ_{H2} are sets of parameters corresponding to PA and pharmaceutical, respectively.

The ratio (Ra) of the PA and each pharmaceutical indicate the affinity between them. The lower the Ra calculated, the greater the affinity. As can be seen in Table 3, the lower Ra value corresponds to Naproxen and PA. This is consistent with a higher tendency of the PA

film to be fouled by this substance as compared to Diclofenac, in agreement with the decrease in the permeance observed.

Comparison with results published in the literature

Table 4 shows different methods of fabricating membranes related with PA/MOF BTFC membranes with the objective of increasing performance in comparison with TFC membranes. It is difficult to compare them because the materials used and the nanofiltrated solutes and solvents are not the same. However, it can be seen that in all cases a high permeance enhancement was obtained, the highest being that obtained in this work.

Several studies have been reported in the literature concerning the removal of pharmaceuticals by nanofiltration using different membrane polymers. For example, Dong et al.[39] synthesized polysulfone TFN membranes using zeolites as fillers obtaining a permeance of 2 $L \cdot m^{-2} \cdot h^{-1} \cdot bar^{-1}$ and a rejection of ≈90% of the tested pharmaceutically active compounds (PhACs). Vergili[40] studied the application of the commercial membrane FM NP010 (polyethersulfone) to the removal of Diclofenac, Ibuprofen and Carbamazepine and obtained a rejection of 88% of Diclofenac with a water permeance of 7 $L \cdot m^{-2} \cdot h^{-1} \cdot bar^{-1}$. Basu et al.[41] incorporated MOF ZIF-8 on a polysulfore support by the layer by layer method and applied the resulting membrane to the nanofiltration of Paracetamol, achieving a rejection of 55% and a permeance of 4 $L \cdot m^{-2} \cdot h^{-1} \cdot bar^{-1}$. Table 5 shows some additional examples of the application of nanofiltration to the removal of Diclofenac and Naproxen.

Table 4: Performance of PA/MOF membranes fabricated using different methods.

Method	MOF	Feed[a]	Permeance ($L \cdot m^{-2} \cdot h^{-1} \cdot bar^{-1}$)	Permeance enhancement[b]	Rejection (%)	Ref.

				(%)		
Layer by Layer	ZIF-8	CR+Water	2.7	142	99.2	[22]
Layer by Layer	ZIF-8	PCM+Water	4	100	55	[41]
Langmuir-Blodgett	MIL-101 (Cr)	SY+MeOH	10.1	35	91.1	[23]
		RB+MeOH	9.5	58	96	
Dip-coating	ZIF-8	SY+MeOH	8.7	50	90	[21]
Evaporation-controlled Filler Positioning (EFP)	ZIF-8	NaCl+Water	2.75	189	83	[24]
Interfacial synthesis	HKUST-1	DIC+Water	33.1	386	99.5	This work
	ZIF-93		*24.2*	*256*	*99*	

[a] CR: Congo red (697 g·mol^{-1}), PCM: Paracetamol (151 g·mol^{-1}), SY: Sunset yellow (450 g·mol^{-1}), RB: Rose bengal (1017 g·mol^{-1}), NaCl: Sodium chloride (58 g·mol^{-1}) and DIC: Diclofenac (296 g·mol^{-1}).

[b] The permeance enhancement was calculated as follows: $\% = \frac{P_{PA/MOF} - P_{TFC}}{P_{TFC}} \cdot \mathbf{100}$

Table 5: Performance of different membranes in the nanofiltration of Diclofenac and/or Naproxen

Membrane	**Drug**	**Permeance (L·m^{-2}·h^{-1}·bar^{-1})**	**Rejection (%)**	**Ref.**
TFN (PA) Zeolite	Diclofenac	2	92	[39]
DOW FILMTEC™ NF270	Diclofenac	10.3	85	[42]
DK (GE Osmonics)	Diclofenac	3.6	71	[42]

FM NP010 (Microdyn-Nadir, GmbH)	Diclofenac	7	88	[40]
Trisep® TS-80	Diclofenac	4.3	89.5	[43]
	Naproxen		89	
Desal HL (GE Osmonics)	Diclofenac	7.2	87.5	[43]
	Naproxen		78	
PA/HKUST-1 BTFC	Diclofenac	33.1	99.5	This work
	Naproxen	24.9	98.3	
PA/ZIF-93 BTFC	Diclofenac	24.2	99	This work
	Naproxen	10.5	99.3	

Stability of Polyamide/HKUST-1 membrane

To check the membrane stability, PA/HKUST-1 BTFC (with which the best results were obtained) and TFC membranes were submitted to 3 nanofiltration cycles using Diclofenac as the solute. Figure 5 shows the percentage of the normalized permeance obtained in each cycle. As can be seen, the decrease in the permeance, mainly caused by fouling, was higher for the TFC membranes than for the PA/HKUST-1 BTFC membranes. Fouling is produced by complex interactions between the membrane surface and the solute dissolved in the feed solution. Two of the factors that come into play in these interactions are the hydrophilic/hydrophobic character of the membrane surface and the electrostatics interactions between this and the solute. [44]

Hydrophobic membranes, with their surfaces more inclined to interact with organic molecules, are more prone to fouling. As Table 2 shows, the introduction of the HKUST-1

layer increased the membrane hydrophilicity, giving rise to a low contact angle of 55º, ca. 20º below that of the TFC membrane. Therefore, there was less fouling and the permeance decrease in each cycle was lower.

However, HKUST-1 has been reported as a material with low stability in water.[31] Presumably, therefore, the duration of the nanofiltration cycles is not long enough for the HKUST-1 to suffer important changes altering the permeance and rejection. This is in agreement with previous works that show that the structure of HKUST-1 is maintained in Mixed Matrix Membranes after 30 h under mild acidic reaction conditions (acetic acid and ethanol esterification) which are more drastic conditions.[33] After the stability experiment, the membrane has been characterized by SEM (Figure S6). Apparently, the MOF retained its layer structure upon nanofiltration at the conditions of the stability experiment; anyway longer tests should be carried out to assess the whole stability of the membrane. On the other hand, ZIFs are known for their hydrothermal stability[45] and, specifically, ZIF-93 has been tested for the adsorption of 5-hydroxymethylfurfural (HMF)[46] and polyols[47] from aqueous solution. Therefore, the PA/ZIF-93 BTFC membrane is a plausible alternative to the PA/HKUST-1 BTFC since, although it has a lower permeation, its stability in water is greater.

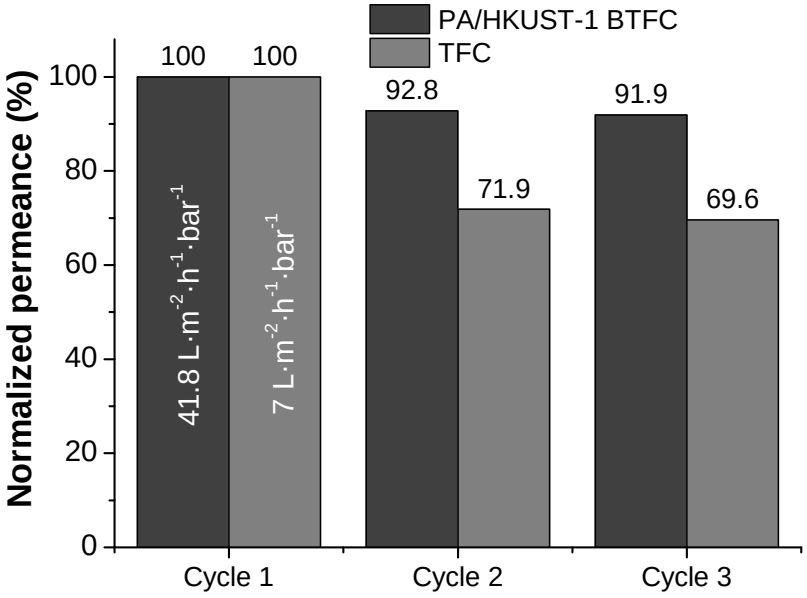

Figure 5: Percentage of the normalized permeance obtained in each cycle with Diclofenac used as solute. Applied pressure 10 bar and temperature 20 ºC.

CONCLUSIONS

The fabrication of PA/MOF BTFC membranes has been carried with HKUST-1 and ZIF-93 MOFs. The MOF layers were prepared via interfacial synthesis on an asymmetric polyimide support of P84®. SEM images before the interfacial polymerization confirmed the formation of the MOF layer over the polymeric support, more homogenous and continuous for HKUST-1 than for ZIF-93. In addition, the SEM images after IP showed that a polyamide layer was correctly synthesized covering completely the MOF layer, thinner in the PA/HKUST-1 BTFC membrane than in the PA/ZIF-93 BTFC. The AFM characterization showed that the membrane roughness followed the order MOF/PA BTFC > TFN MOF > TFC membranes, being higher with the MOF HKUST-1. FTIR-ATR

confirmed the presence of the crystalline MOFs over the P84® support and the conservation of their structure during the IP process.

Compared to TFC and TFN (with nanoparticles of MOFs dispersed in the polyamide layer), PA/MOF BTFC membranes improved their performance during the Diclofenac and Naproxen aqueous solution nanofiltration thanks to the MOF porosity, membrane hydrophilicity, PA layer thickness and membrane roughness. The best results were obtained with PA/HKUST-1 BTFC with a water permeance increased, as compared to the TFC performance, from 6.8 $L \cdot m^{-2} \cdot h^{-1} \cdot bar^{-1}$ to 33.1 $L \cdot m^{-2} \cdot h^{-1} \cdot bar^{-1}$ and from 4.3 $L \cdot m^{-2} \cdot h^{-1} \cdot bar^{-1}$ to 24.9 $L \cdot m^{-2} \cdot h^{-1} \cdot bar^{-1}$ for Diclofenac and Naproxen aqueous solution, respectively, with rejections over 98%.

The interactions between the pharmaceuticals and the membrane surface have been assessed in terms of Hansen solubility parameters, showing a better affinity of the membrane surface with Naproxen which explains the lower permeances obtained in its nanofiltration. The stability of PA/HKUST-1 BTFC and TFC membranes was studied by submitting them to three Diclofenac nanofiltration cycles. The greater hydrophilic character of HKUST-1 provided anti-fouling properties to the membrane and, therefore, a lower decrease in the permeance due to fouling.

ASSOCIATED CONTENT

Supporting Information

Experimental details, XRD, SEM, TGA, FTIR-ATR, nanofiltration results. This material is available free of charge via the Internet at http://pubs.acs.org.

AUTHOR INFORMATION

Corresponding Author:

*ctellez@unizar.es

Author Contributions

All authors have given approval to the final version of the manuscript.

ACKNOWLEDGMENTS

Financial support from the Spanish MINECO and FEDER (MAT2016-77290-R), the Aragón Government (T43-17R) and the ESF is gratefully acknowledged. L. P. thanks the Spanish Ministry of Economy, Industry and Competitiveness Program FPI2014 for her PhD grant. All the microscopy work was done in the Laboratorio de Microscopías Avanzadas at the Instituto de Nanociencia de Aragón (LMA-INA). Finally, the authors would like to acknowledge the use of the Servicio General de Apoyo a la Investigación-SAI, Universidad de Zaragoza. Prof. Dr Steven Abbott is thanked for providing Hansen solubility parameters.

ABBREVIATIONS

AFM: Atomic Force Microscope, ATR-FTIR: Attenuated total reflection Fourier transform infrared spectroscopy, BET: Brunauer-Emmett-Teller method, BTFC: Bilayered Thin Film Composite, DMSO: Dimethylsulfoxide HDA: hexanediamine, HKUST-1: Hong Kong University of Science and Technology, IP: interfacial polymerization, IPA: isopropyl alcohol, MOF: metal-organic framework, MPD: m-phenylenediamine, PA: polyamide, PEG: polyethylene glycol, PI: polyimide, R_a: roughness average, RMS: root mean square,

SEM: scanning electron microscopy, TFC: thin film composite, TFN: thin film nanocomposite, TGA: thermogravimetric analysis, TMC: trimesoyl chloride, XRD: x-ray diffraction, WWTP: wastewater treatment plant, ZIF: Zeolitic imidazolate frameworks.

REFERENCES

(1) Silva, B. F. d.; Jelic, A.; López-Serna, R.; Mozeto, A. A.; Petrovic, M.; Barceló, D., Occurrence and distribution of pharmaceuticals in surface water, suspended solids and sediments of the Ebro river basin, Spain. *Chemosphere* **2011,** *85* (8), 1331-1339.
(2) Petrović, M.; Gonzalez, S.; Barceló, D., Analysis and removal of emerging contaminants in wastewater and drinking water. *Trends Anal. Chem.* **2003,** *22* (10), 685-696.
(3) Bolong, N.; Ismail, A. F.; Salim, M. R.; Matsuura, T., A review of the effects of emerging contaminants in wastewater and options for their removal. *Desalination* **2009,** *239* (1), 229-246.
(4) Fent, K.; Weston, A. A.; Caminada, D., Ecotoxicology of human pharmaceuticals. *Aquat. Toxicol.* **2006,** *76* (2), 122-159.
(5) Gros, M.; Petrović, M.; Ginebreda, A.; Barceló, D., Removal of pharmaceuticals during wastewater treatment and environmental risk assessment using hazard indexes. *Environment International* **2010,** *36* (1), 15-26.
(6) Wintgens, T.; Salehi, F.; Hochstrat, R.; Melin, T., Emerging contaminants and treatment options in water recycling for indirect potable use. *Water Sci. Technol.* **2008,** *57* (1), 99-107.
(7) Taheran, M.; Brar, S. K.; Verma, M.; Surampalli, R. Y.; Zhang, T. C.; Valero, J. R., Membrane processes for removal of pharmaceutically active compounds (PhACs) from water and wastewaters. *Sci. Total Environ.* **2016,** *547*, 60-77.
(8) Buonomenna, M. G.; Bae, J., Organic Solvent Nanofiltration in Pharmaceutical Industry. *Sep. Purif. Rev.* **2015,** *44* (2), 157-182.
(9) Nath, K.; Dave, H. K.; Patel, T. M., Revisiting the recent applications of nanofiltration in food processing industries: Progress and prognosis. *Trends Food Sci. Technol.* **2018,** *73*, 12-24.
(10) Gozálvez-Zafrilla, J. M.; Sanz-Escribano, D.; Lora-García, J.; León Hidalgo, M. C., Nanofiltration of secondary effluent for wastewater reuse in the textile industry. *Desalination* **2008,** *222* (1), 272-279.
(11) Ge, S.; Feng, L.; Zhang, L.; Xu, Q.; Yang, Y.; Wang, Z.; Kim, K.-H., Rejection rate and mechanisms of drugs in drinking water by nanofiltration technology. *EER* **2017,** *22* (3), 329-338.
(12) Vandezande, P.; Gevers, L. E. M.; Vankelecom, I. F. J., Solvent resistant nanofiltration: separating on a molecular level. *Chem. Soc. Rev.* **2008,** *37* (2), 365-405.
(13) Van der Bruggen, B.; Vandecasteele, C., Removal of pollutants from surface water and groundwater by nanofiltration: overview of possible applications in the drinking water industry. *Environ. Pollut.* **2003,** *122* (3), 435-445.

(14) Jeong, B.-H.; Hoek, E. M. V.; Yan, Y.; Subramani, A.; Huang, X.; Hurwitz, G.; Ghosh, A. K.; Jawor, A., Interfacial polymerization of thin film nanocomposites: A new concept for reverse osmosis membranes. *J. Membr. Sci.* **2007,** *294* (1–2), 1-7.
(15) Ma, N.; Wei, J.; Liao, R.; Tang, C. Y., Zeolite-polyamide thin film nanocomposite membranes: Towards enhanced performance for forward osmosis. *J. Membr. Sci.* **2012,** *405-406*, 149-157.
(16) Echaide-Gorriz, C.; Sorribas, S.; Tellez, C.; Coronas, J., MOF nanoparticles of MIL-68(Al), MIL-101(Cr) and ZIF-11 for thin film nanocomposite organic solvent nanofiltration membranes. *RSC Adv.* **2016,** *6* (93), 90417-90426.
(17) Bano, S.; Mahmood, A.; Kim, S.-J.; Lee, K.-H., Graphene oxide modified polyamide nanofiltration membrane with improved flux and antifouling properties. *J. Mater. Chem. A* **2015,** *3* (5), 2065-2071.
(18) Lee, H. S.; Im, S. J.; Kim, J. H.; Kim, H. J.; Kim, J. P.; Min, B. R., Polyamide thin-film nanofiltration membranes containing TiO2 nanoparticles. *Desalination* **2008,** *219* (1), 48-56.
(19) Ferey, G., Hybrid porous solids: past, present, future. *Chem. Soc. Rev.* **2008,** *37* (1), 191-214.
(20) Sorribas, S.; Gorgojo, P.; Téllez, C.; Coronas, J.; Livingston, A. G., High Flux Thin Film Nanocomposite Membranes Based on Metal–Organic Frameworks for Organic Solvent Nanofiltration. *J. Am. Chem. Soc.* **2013,** *135* (40), 15201-15208.
(21) Sarango, L.; Paseta, L.; Navarro, M.; Zornoza, B.; Coronas, J., Controlled deposition of MOFs by dip-coating in thin film nanocomposite membranes for organic solvent nanofiltration. *J. Ind. Eng. Chem.* **2018,** *59*, 8-16.
(22) Wang, L.; Fang, M.; Liu, J.; He, J.; Li, J.; Lei, J., Layer-by-Layer Fabrication of High-Performance Polyamide/ZIF-8 Nanocomposite Membrane for Nanofiltration Applications. *ACS Appl. Mater. Interfaces* **2015,** *7* (43), 24082-24093.
(23) Navarro, M.; Benito, J.; Paseta, L.; Gascón, I.; Coronas, J.; Téllez, C., Thin-Film Nanocomposite Membrane with the Minimum Amount of MOF by the Langmuir–Schaefer Technique for Nanofiltration. *ACS Appl. Mater. Interfaces* **2018,** *10* (1), 1278-1287.
(24) Van Goethem, C.; Verbeke, R.; Hermans, S.; Bernstein, R.; Vankelecom, I. F. J., Controlled positioning of MOFs in interfacially polymerized thin-film nanocomposites. *J. Mater. Chem. A* **2016,** *4* (42), 16368-16376.
(25) Cacho-Bailo, F.; Caro, G.; Etxeberría-Benavides, M.; Karvan, O.; Téllez, C.; Coronas, J., High selectivity ZIF-93 hollow fiber membranes for gas separation. *Chem. Commun. (Cambridge, U. K.)* **2015,** *51* (56), 11283-11285.
(26) Chui, S. S.-Y.; Lo, S. M.-F.; Charmant, J. P. H.; Orpen, A. G.; Williams, I. D., A Chemically Functionalizable Nanoporous Material [Cu3(TMA)2(H2O)3]n. *Science* **1999,** *283* (5405), 1148-1150.
(27) Carmona, E.; Andreu, V.; Picó, Y., Occurrence of acidic pharmaceuticals and personal care products in Turia River Basin: From waste to drinking water. *Sci. Total Environ.* **2014,** *484*, 53-63.
(28) Houtman, C. J.; Kroesbergen, J.; Lekkerkerker-Teunissen, K.; van der Hoek, J. P., Human health risk assessment of the mixture of pharmaceuticals in Dutch drinking water and its sources based on frequent monitoring data. *Sci. Total Environ.* **2014,** *496*, 54-62.

(29) Liu, X.; Li, Y.; Ban, Y.; Peng, Y.; Jin, H.; Bux, H.; Xu, L.; Caro, J.; Yang, W., Improvement of hydrothermal stability of zeolitic imidazolate frameworks. *Chem. Commun. (Cambridge, U. K.)* **2013,** *49* (80), 9140-9142.
(30) Wee, L. H.; Lohe, M. R.; Janssens, N.; Kaskel, S.; Martens, J. A., Fine tuning of the metal-organic framework Cu3(BTC)2 HKUST-1 crystal size in the 100 nm to 5 micron range. *J. Mater. Chem.* **2012,** *22* (27), 13742-13746.
(31) Campbell, J.; Davies, R. P.; Braddock, D. C.; Livingston, A. G., Improving the permeance of hybrid polymer/metal-organic framework (MOF) membranes for organic solvent nanofiltration (OSN) - development of MOF thin films via interfacial synthesis. *J. Mater. Chem. A* **2015,** *3* (18), 9668-9674.
(32) Jimenez Solomon, M. F.; Bhole, Y.; Livingston, A. G., High flux membranes for organic solvent nanofiltration (OSN)—Interfacial polymerization with solvent activation. *J. Membr. Sci.* **2012,** *423–424*, 371-382.
(33) Sorribas, S.; Kudasheva, A.; Almendro, E.; Zornoza, B.; de la Iglesia, Ó.; Téllez, C.; Coronas, J., Pervaporation and membrane reactor performance of polyimide based mixed matrix membranes containing MOF HKUST-1. *Chem. Eng. Sci.* **2015,** *124*, 37-44.
(34) Namvar-Mahboub, M.; Pakizeh, M.; Davari, S., Preparation and characterization of UZM-5/polyamide thin film nanocomposite membrane for dewaxing solvent recovery. *J. Membr. Sci.* **2014,** *459*, 22-32.
(35) Toyao, T.; Liang, K.; Okada, K.; Ricco, R.; Styles, M. J.; Tokudome, Y.; Horiuchi, Y.; Hill, A. J.; Takahashi, M.; Matsuoka, M.; Falcaro, P., Positioning of the HKUST-1 metal–organic framework (Cu3(BTC)2) through conversion from insoluble Cu-based precursors. *Inorganic Chemistry Frontiers* **2015,** *2* (5), 434-441.
(36) Silverstein, R. M.; Webster, F. X.; Kiemle, D. J.; Bryce, D. L., *Spectrometric Identification of Organic Compounds*. Wiley: 2014.
(37) Hansen, C. M., 50 Years with solubility parameters—past and future. *Prog. Org. Coat.* **2004,** *51* (1), 77-84.
(38) Bustamante, P.; Peña, M. A.; Barra, J., Partial-solubility Parameters of Naproxen and Sodium Diclofenac. *J. Pharm. Pharmacol.* **1998,** *50* (9), 975-982.
(39) Dong, L.-x.; Huang, X.-c.; Wang, Z.; Yang, Z.; Wang, X.-m.; Tang, C. Y., A thin-film nanocomposite nanofiltration membrane prepared on a support with in situ embedded zeolite nanoparticles. *Sep. Purif. Technol.* **2016,** *166*, 230-239.
(40) Vergili, I., Application of nanofiltration for the removal of carbamazepine, diclofenac and ibuprofen from drinking water sources. *J. Environ. Manage.* **2013,** *127*, 177-187.
(41) Basu, S.; Balakrishnan, M., Polyamide thin film composite membranes containing ZIF-8 for the separation of pharmaceutical compounds from aqueous streams. *Sep. Purif. Technol.* **2017,** *179*, 118-125.
(42) Bohdziewicz, J.; Kudlek-Jelonek, E.; Dudziak, M., Removal of selected pharmaceutical compounds form the simulated municipal secondary effluent using the nanofiltration process. In *Monographs of the Environmental Engineering Commitee Polish Academy of Sciences: Membranes and Membranes Processes in Environmental Protection*, Bodzek, M.; Pelczar, J., Eds. Polska Akademia Nauk. Komitet Inżynierii Środowiska: 2014; Vol. 119, pp 219-228.

(43) Verliefde, A. R. D.; Cornelissen, E. R.; Heijman, S. G. J.; Petrinic, I.; Luxbacher, T.; Amy, G. L.; Van der Bruggen, B.; van Dijk, J. C., Influence of membrane fouling by (pretreated) surface water on rejection of pharmaceutically active compounds (PhACs) by nanofiltration membranes. *J. Membr. Sci.* **2009,** *330* (1), 90-103.
(44) Mashallah Rezakazemi, A. D., Riasat Harami Hossein, Nasibeh Hajilari and Inamuddin, Fouling-resistant membranes for water reuse. *Environ. Chem. Lett.* **2018,** *16* (3), 715-763.
(45) Wang, C.; Liu, X.; Keser Demir, N.; Chen, J. P.; Li, K., Applications of water stable metal–organic frameworks. *Chem. Soc. Rev.* **2016,** *45* (18), 5107-5134.
(46) Jin, H.; Li, Y.; Liu, X.; Ban, Y.; Peng, Y.; Jiao, W.; Yang, W., Recovery of HMF from aqueous solution by zeolitic imidazolate frameworks. *Chem. Eng. Sci.* **2015,** *124*, 170-178.
(47) Jin, H.; Li, Y.; Yang, W., Adsorption of Biomass-Derived Polyols onto Metal–Organic Frameworks from Aqueous Solutions. *Ind. Eng. Chem. Res.* **2018,** *57* (35), 11963-11969.

TABLE OF CONTENTS (TOC)/ABSTRACT GRAPHICS

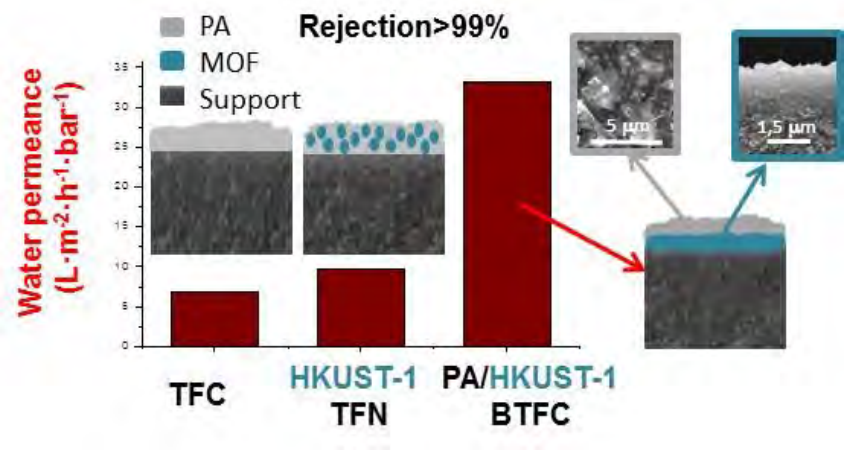

Polyamide/MOF Bilayered Thin Film Composite Membranes for the Removal of Pharmaceutical Compounds from Water have been developed.